

# BUNDL: Bayesian Uncertainty-aware Deep Learning with Noisy training Labels for Seizure Detection in EEG

Deeksha M. Shama, *Student, IEEE*, Archana Venkataraman, *Senior Member, IEEE*

**Abstract**—Objective: Deep learning methods are at the forefront of automated epileptic seizure detection and onset zone localization using scalp-EEG. However, the performance of deep learning methods rely heavily on the quality of annotated training datasets. Scalp EEG is susceptible to high noise levels, which in turn leads to imprecise annotations of the seizure timing and characteristics. This “label noise” presents a significant challenge in model training and generalization. In this paper, we introduce a novel statistical framework that informs a deep learning model of label ambiguity, thereby enhancing the overall seizure detection performance. Methods: Our Bayesian Uncertainty-aware Deep Learning (BUNDL) strategy offers a straightforward and model-agnostic method for training deep neural networks with noisy training labels that does not add any parameters to existing architectures. By integrating domain knowledge into the statistical framework, we derive a novel KL-divergence-based loss function that capitalizes on uncertainty to better learn seizure characteristics from scalp EEG. Additionally, we explore the impact of improved seizure detection on the task of automated onset zone localization. Results: We validate BUNDL using a comprehensive simulated EEG dataset and two publicly available datasets collected Temple University Hospital (TUH) and Boston Children’s Hospital (CHB-MIT). BUNDL consistently improves the performance of three base models on simulated data under seven types of label noise and three EEG signal-to-noise ratios. Similar improvement were observed in the real-world TUH and CHB-MIT datasets. Finally, we demonstrate that BUNDL improves the accuracy of seizure onset zone localization. Conclusion: We have presented BUNDL, a novel method to handle noisy annotations that are common in EEG datasets of epilepsy. Our method can be seamlessly integrated with existing deep models used in clinical practice. Significance: Although deep learning models exist for seizure detection, there is a need for a training framework tailored to the complexities of EEG data. BUNDL is specifically designed to address label ambiguities, enabling the training of reliable and trustworthy models for epilepsy evaluation.

**Index Terms**—Bayesian Deep Learning, Epilepsy, EEG, Seizure Detection, Learning under Noisy Training Labels

## I. INTRODUCTION

Epilepsy is a debilitating neurological disorder characterized by recurring seizures. Drug-resistant epileptic patients typically require further evaluation to determine an appropriate treatment plan, such as surgical resection of a focal lesion. Scalp EEG is the first and foremost modality used for assessing epileptic patients. This evaluation involves days-long EEG monitoring to identify abnormalities, such as epileptiform discharges, that indicate the time(s) and location(s) of seizure activity. EEG also presents as a natural choice for presurgical planning complimented with MRI due to its non-invasiveness, affordability, and ease of acquisition. However, EEG signals are complex and susceptible to artifacts; hence, the

“This work was supported by the National Institutes of Health R01 EB029977 (PI Caffo), the National Institutes of Health R01 HD108790 (PI Venkataraman), and the National Institutes of Health R21 CA263804 (PI Venkataraman).”

D. M. Shama is with the Johns Hopkins University, Baltimore, MD 21218 USA and Boston University, Boston, MA 02215 USA (e-mail: dshama1@jhu.edu).

A. Venkataramans was with the Johns Hopkins University, Baltimore, MD 21218 USA and is now with Boston University, Boston, MA 02215 USA (e-mail: archanav@bu.edu).

manual review of this data is both labor-intensive and prone to error. To address these challenges, various computer-aided models have been developed, with deep learning models recently demonstrating remarkable success in seizure detection and characterization.

Despite this progress, most deep learning models for seizure detection are based on a supervised learning paradigm, which uses a *training dataset* of EEG recordings and “ground truth” labels of seizure activity annotated by clinicians to learn salient features that can be generalized to new data. Promisingly, deep learning models are highly capable of extracting relevant features in complex and high dimensional data during training under the assumption that the provided “ground truth” labels are accurate. Unfortunately, clinician-annotated labels of seizure activity can suffer from manual error and poor inter-rater reliability. Research has shown that the inter-rater agreement among clinicians interpreting EEG data hovers around 60%, underscoring the inconsistency in annotations [1], [2]. Another study attributed this variability largely to differing decision thresholds among clinicians [3], particularly in epilepsy, where a lower threshold is often adopted to minimize the risk of missing seizures, leading to over-segmentation of seizures and misdiagnosis of epilepsy [4]. When AI models are trained without considering such label ambiguities, they may learn misleading features, resulting in poor generalizability. In fact, previous studies have suggested that the performance of AI models may plateau on widely used datasets like the Temple University Hospital Corpus due to this variability [5]. Thus, there is a need for robust, noise-aware deep learning frameworks that can enhance the reliability of automated seizure detection systems.

## A. Automated Seizure Detection and Onset Zone Localization

Automated seizure detection has been an active area of research for the past three decades. Traditionally, seizure detection algorithms have followed a three-stage pipeline: (i) signal preprocessing and segmentation into short pseudo-stationary time windows, (ii) extraction of discriminatory features, and (iii) classifying each window as either baseline or seizure activity. To date, the bulk of prior work has focused on feature extraction. In the simplest case, singular features, such as spike count [6] and signal statistics, such as power, skewness, kurtosis, and maximum amplitude [7], were used to summarize the EEG in each time window. However, it was quickly discovered that these features were not robust, as several inter-ictal (non-seizure) artifacts could also resemble seizure. Hence, researchers explored more complex features to overcome this challenge, such as non-linear dynamics [8], hidden Markov models [9], frequency domain features using Fourier transform such as power spectral density [10] and short-time Fourier transform [11], wavelet domain features [12] and graph theoretic features [13]. Finally, several machine learning classifiers have been explored for seizure detection, such as support vector machines [8], [10], [11], logistic regression [11], Bayes [11], random forests and decision trees [6], [10], and multi-layer perceptrons [11]. While they represent seminal contributions to the field, traditional approaches perform best on group-level analyses and often fail to capture patient-specific features and to generalize to unseen patients.

In contrast, recent deep learning methods have demonstrated the capacity to extract data-driven features from complex and high-dimensional training dataset and successfully apply them to unseen

patients. For example, convolutional neural networks (CNNs) consist of multiple layers with small kernels to extract features within a local field of view and can be used to aggregate information across multiple EEG channels. A variety of CNN-based models have been developed for seizure detection from EEG data. These models include 1D CNNs that operate across time [14], 2D CNNs that fuse information across time and EEG channels [15], 3D CNNs that add frequency-domain analysis [16], [17], graph CNNs to incorporate channel neighborhood information [18], and state-of-art temporal graph CNNs [19]. While CNNs effectively capture spatial correlations between EEG channels, they operate on short time-scales with limited memory of past events. Consequently, researchers have adopted recurrent neural networks [20], [21] and LSTM units [22] to capture seizure progression, either independently or in conjunction with CNN encoders [23]. Finally, transformers are recent class models that use a self-attention mechanism for feature extraction [24]–[27] and can effectively capture multi-level spatio-temporal correlations in EEG data to identify seizures. Despite differences in the deep neural network architectures, all of these methods are trained in a supervised manner. Specifically, they use clinician-annotated training data, consisting of EEG recordings and “ground truth” labels of the seizure interval, to learn the model parameters. This process is done by minimizing a cross-entropy loss (CEL) between the model predictions of baseline versus seizure activity and the clinician-provided training labels. By design, this training strategy assumes that the given seizure labels are accurate and cannot handle ambiguities in the annotated seizure intervals. This assumption has contributed to poor generalization across heterogeneous patient cohorts [5].

## B. Learning with Label Noise

The challenge of training with ambiguous or inaccurate labels is gaining traction within the deep learning community. Early approaches focus on eliminating noisy samples from the training dataset using either domain knowledge or prior information about the task. For example, the work of [28] uses pretrained network parameters to assess data quality by identifying samples with highest loss. These samples are removed, and the model is retrained on clean samples. Similarly, the work of [29] incorporates a neighborhood constraint to ensure smooth sample rejection by leveraging data correlations. Finally, the method of [30] introduces confidence learning, in which confusion matrices from pretrained networks are employed to differentiate between clean and noisy labels before removal. These “hard pruning” strategies are entirely dependent on the accuracy of the pretrained network and can erroneously keep/reject samples. In contrast, “soft pruning” adjusts the loss function during retraining to control how much the model learns from each sample based on its noise level, while also addressing the class imbalance common in medical datasets [31]. One drawback of pruning strategies is that the “outside information” used to obtain an accurate pretrained network is often unavailable in real-world applications. A second drawback is that in complex modalities like EEG, all samples may appear equally noisy, leading to the potential removal of key samples or, in an extreme case, the rejection of the entire dataset.

The second set of approaches introduce novel architectural changes to deep neural networks that aim to decipher a set of “clean labels” from the noisy training data. For instance, the work of [32] elegantly addresses the learning challenge by adding a noise adaptation layer on top of an existing architecture. This layer models the transition from clean to noisy labels and draws inspiration from the expectation-maximization (EM) estimation procedure for inferring posterior probability distributions. Building on this concept, other works combine noise adaptation layers with confusion matrix-guided estimation of

label transitions while also incorporating optimization constraints into the loss function to enhance robustness [33], [34]. However, the parameters introduced by these methods scale with the square of the number of predicted classes,  $O(n^2)$ . In addition, these methods generally require a computationally intensive multi-stage training procedure that makes strong assumptions about the clean labels, further complicating their practical application. [35]–[39].

Yet another strategy has been the development of novel loss functions to algorithmically learn the clean label posterior. For example, self-supervised methods like [40] update the class confidence based on past predictions; however, they assume class-conditional noise and often overlook confounding factors from the input, which is common in complex data like EEG. Unsupervised methods, such as [41], employ mix-up data augmentation and bootstrapping to estimate clean labels based on the principle that a linear combination of inputs should imply a linear combination in class probabilities. However, the assumption of linear data variations may not be appropriate for complex modalities like EEG. Assumption-free approaches offer a more flexible way to handle label noise by creating novel loss functions [42], [43], but they still struggle to model input data-dependent label transitions, which are crucial for dealing with complex data.

Finally, previous research on seizure detection from EEG has made significant strides by denoising the signals to improve prediction accuracy [44]. There has also been valuable work in quantifying uncertainty in predictions using techniques like Monte Carlo dropout [45], [46]. Some studies incorporate synthetic label noise addition [47] and annotations from multiple clinicians [48], [49]. Unfortunately, these approaches do not fully address the underlying challenges of learning with noisy labels without increasing the need for (costly) manual effort and/or computational overhead.

## II. OUR CONTRIBUTIONS

We introduce BUNDL, a novel approach to handling instance-dependent label noise in EEG-based seizure detection using Bayesian modeling. BUNDL is designed specifically for the complexity of EEG data and seizure detection; it can be optimized directly from clinician-provided training labels, with the flexibility to incorporate multi-annotator information when available. Our key contribution lies in developing a distributional loss function that captures the complex transitions from clean to noisy labels *without adding any parameter overhead to the current deep network architecture*. To enhance the reliability of our predictions, we use Monte Carlo dropout to estimate uncertainty, allowing us to adjust the posterior probabilities of label flips dynamically. This work was introduced as short paper at the UNSURE workshop of MICCAI 2024. Here, we further validate our approach via experiments on a comprehensive simulated EEG dataset with seven types of label noise and three signal-to-noise ratios. Additionally, we evaluate our method on two real-world EEG datasets, showing not only interpretable results but also enhanced seizure onset zone localization in a secondary analysis. Importantly, BUNDL can be used to train *any deep learning model*, and while it is tailored for EEG, it can be easily extend to other modalities.

## III. METHODS AND MATERIALS

### A. BUNDL: Bayesian Uncertainty aware Deep Learning

Our Bayesian UNcertainty aware Deep Learning (BUNDL) framework distinguishes between noisy and clean labels via the graphical model illustrated in Fig 1. Specifically, we model the observed sample (in our case short EEG windows), represented by the random variable  $x$ , as dependent on the *unobserved* clean labels  $y$ . Formally,  $y$  is a binary random variable that indicates the presence or absence of true seizure activity. The noisy training label  $\hat{y}$  (often provided by

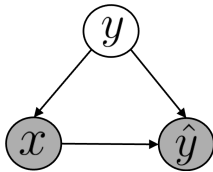


Fig. 1: Directed graphical model depicting the relationships between random variables  $x$  (EEG input),  $y$  (clean label),  $\hat{y}$  (noisy label). The arrows imply a probabilistic dependency between variables.

clinicians) is also a binary random variable, but it is influenced by both the observed EEG data  $x$  and the true seizure label  $y$ . During training,  $\hat{y}$  is available for the model to use for optimization, while  $y$  remains unknown. During testing, the model relies solely on the learned parameters without access to any annotations. In simulated experiments, we set aside  $y$  to evaluate the model, using  $\hat{y}$  for real-world datasets like TUH and CHB-MIT, where clean annotations are unavailable. Finally, the graphical model assumes an instantaneous relationship between variables, meaning the noise corruption of a particular label does not depend on past or future time points.

**1) Overview:** Our high-level strategy is to recognize that the training labels of seizure activity, derived from clinical review of the EEG, may be unreliable when the data contains significant noise or artifacts. Thus, we develop a statistical framework that models the mismatch between the given labels  $\hat{y}$  and the (unseen) ground truth labels  $y$ , which we refer to as “clean” labels. Based on this framework, we learn the function  $f_\theta(\cdot)$ , parameterized by a deep neural network parameter  $\theta$ , infer the clean label posterior distribution  $p(y|x)$  given the EEG data  $x$  in a partially self-supervised manner. This strategy allows us to predict true seizure activity given noisy annotations during training. Note that  $\theta$  can refer to any deep network that incorporates dropout, making BUNDL model-agnostic.

Formally, given the training EEG data and seizure versus baseline labels  $(x, \hat{y})$ , we define the noisy label posterior distribution as  $p(\hat{y}|x) = \mathcal{B}(\hat{y}; p_g)$ , where  $\mathcal{B}(\cdot)$  denotes a Bernoulli distribution, and the parameter  $p_g$  denotes the probability of seizure activity. In our case,  $p_g$  equals the binary label of seizure activity provided by the clinician, but it could alternatively equal a continuous measure of clinician confidence, should that information be available. We account for the mismatch between the unknown label  $y$  and the observed label  $\hat{y}$  for the given EEG window  $x$  as follows:

$$p(y|x, \hat{y}) = \mathcal{B}(y; p_g(1 - z_x^{\hat{y}}) + \overline{f_\theta(x)} z_x^{\hat{y}}), \quad (1)$$

where  $z_x^{\hat{y}}$  is the data uncertainty and  $\overline{f_\theta(x)}$  is the average of multiple model predictions  $f_\theta(\cdot)$  that are computed using Monte-Carlo dropout in the deep network, as described in the next subsection. Intuitively, when the uncertainty  $z_x^{\hat{y}}$  is low, the model trusts the given labels  $p_g$ , as the accuracy of manual annotations of seizure activity is considered reliable. In contrast, when the uncertainty  $z_x^{\hat{y}}$  is high, the model hinges towards its self-supervision  $\overline{f_\theta(x)}$  and ignores the given labels.

We multiply Eq. (1) with  $p(\hat{y}|x) = \mathcal{B}(\hat{y}; p_g)$  to obtain the joint distribution  $p(y, \hat{y}|x)$ . From here, we marginalize  $\hat{y}$  from the joint to obtain the clean label posterior  $p(y|x) = \mathcal{B}(y; p_{yc})$  as follows:

$$p(y|x) = \sum_{\hat{y}=0}^1 p(y|x, \hat{y}) p(\hat{y}|x)$$

$$p(y|x) = \underbrace{\sum_{\hat{y}=0}^1 \mathcal{B}(y; p_g(1 - z_x^{\hat{y}}) + \overline{f_\theta(x)} z_x^{\hat{y}}) \cdot \mathcal{B}(\hat{y}; p_g)}_{\mathcal{B}(y; p_{yc})}$$

where the clean Bernoulli parameter  $p_{yc}$  can be computed as

$$p_{yc} = p_g(z_x^1 \cdot \overline{f_\theta(x)} + p_g(1 - z_x^1)) + (1 - p_g)(z_x^0 \cdot \overline{f_\theta(x)} + p_g(1 - z_x^0)) \quad (2)$$

During training, we learn the optimal deep network parameters  $\theta^*$  that minimizes the KL divergence between the Bernoulli distribution parameterized by  $p_{yc}$  in Eq. (2) and the deep network prediction  $Q(y|x; \theta) = \mathcal{B}(y; f_\theta(x))$  parameterized by the output  $f_\theta(x)$ :

$$\theta^* = \arg \min_{\theta} D_{KL}(P||Q)$$

$$= \arg \max_{\theta} \left( p_{yc} \cdot \log(f_\theta(x)) + (1 - p_{yc}) \cdot \log(1 - f_\theta(x)) \right)$$

The learned parameters  $\theta^*$  are used to directly estimate the clean label posterior. Thus, our training process aligns the predicted distribution with the true underlying distribution of the clean labels.

**2) Uncertainty Estimation:** The BUNDL training procedure requires the average model prediction  $\overline{f_\theta(x)}$  and the uncertainty  $z_x^{\hat{y}}$  to be computed in every epoch step for all inputs  $x$ . This approach is more flexible than prior work, which used a fixed uncertainty level [40]. We propose using Monte Carlo (MC) dropout for uncertainty estimation, which enables us to compute uncertainty from the existing deep network architecture without adding new parameters. Our approach leverages MC dropout during both training and inference to capture the variability in predictions, thus providing insights into the confidence and the reliability of the model outputs. As shown in Fig. 2, we use dropout to make multiple predictions and estimate an empirical distribution for  $p(y|x)$ . We then compute the uncertainty  $z_x^{\hat{y}}$  as the self-entropy across  $N = 20$  MC samples as

$$z_x^{\hat{y}} = \frac{-1}{CN} \sum_{n=1}^N \bar{f}^n \log \bar{f}^n + (1 - \bar{f}^n) \log(1 - \bar{f}^n) \quad (3)$$

The division by  $C = \log(2)$  scales all values to lie between 0 and 1 and the variable  $\bar{f}^n$  corresponds to multiple predictions from the model using the randomization provided by dropout i.e., MC dropout. Our use of MC samples for self-supervision in Eq. (3) is akin to having multiple seizure labels from different clinicians. This strategy mitigates the influence of faulty predictions on the learning process.

Eq. (3) allows us to incorporate *a priori* knowledge about the expected label noise. For example, if we expect both seizure and non-seizure labels to have the same level of uncertainty, then we would set  $z_x^0 = z_x^1$ , as currently shown in Eq. (3). However, it is often the case that clinicians oversegment the seizures to avoid missing problematic time intervals [4]. To accommodate this tendency, we fix  $z_x^0 = 0.001$ , a small quantity, while  $z_x^1$  is derived from Eq. (3). Conversely, if seizures are known to be under-segmented, we could fix  $z_x^1$  at a small value while estimating  $z_x^0$  during training. Hence, the user can adapt BUNDL to different datasets and application domains based on the presumed noise characteristics.

The uncertainty in Eq. 3 reflects both epistemic (model) and aleatoric (data) uncertainty. Our focus is on aleatoric uncertainty, as captured by label mismatch. Without any training,  $z_x^{\hat{y}}$  would be dominated by epistemic uncertainty, and the self-supervision  $\overline{f_\theta(x)}$  would be unreliable [28]. To address this issue, we pretrain the base network using a cross-entropy loss on EEG samples that lie squarely within baseline and seizure regions. In this case, we are more certain that the clinician annotated labels are correct, as ambiguity tends to be highest around the seizure onset and offset times. This pretraining increases model confidence and encourages the uncertainty computed in Eq. (3) to reflect the desired aleatoric uncertainty.

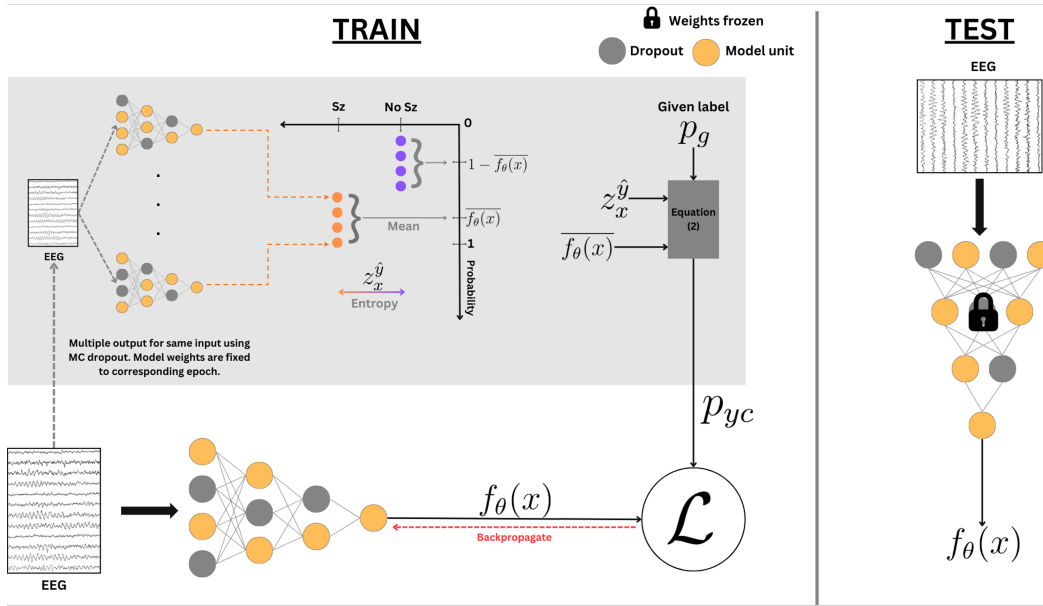


**Fig. 2: Right:** Overall training strategy of BUNDL. For every input EEG sample, we estimate uncertainty using MC dropout, as shown in the top pane. This information augments the standard prediction and backpropagation procedure via the BUNDL loss function, which is depicted in the bottom pane. **Left:** Testing pipeline for evaluating clean label prediction post training.

#### Algorithm 1 BUNDL Training Framework

**Require:** Learning rate  $\alpha$ , Max epochs  $M$ ,  $\{x, p_g\}$  batched data

- 1:  $\theta \leftarrow \theta_{pre}$  {Pretrained model}
- 2:  $m \leftarrow 1$
- 3: **while**  $m \leq M$  **do**
- 4:   **for**  $(x, p_g) \in$  train data **do**
- 5:     Predict  $f_{\theta}(x)$ ,  $\bar{f}_{\theta}(x)$ , and  $z_x^{\hat{y}}$  using Algorithm 2
- 6:      $p_{yc} \leftarrow p_g \cdot (z_x^1 \cdot f_{\theta}(x) + p_g \cdot (1 - z_x^1)) + (1 - p_g) \cdot (z_x^0 \cdot \bar{f}_{\theta}(x) + p_g \cdot (1 - z_x^0))$
- 7:      $\mathcal{L} \leftarrow p_{yc} \cdot \log(f_{\theta}(x)) + (1 - p_{yc}) \cdot \log(1 - f_{\theta}(x))$
- 8:      $\theta \leftarrow \theta - \alpha \nabla \mathcal{L}$  {Update with optimizer}
- 9:   **end for**
- 10:    $m \leftarrow m + 1$
- 11: **end while**

3) **Training Algorithms:** Following the pretraining phase, we utilize procedure outlined in Algorithm 1 and Fig 2 to train the deep network augmented with BUNDL. Each training epoch includes making a prediction, computing the uncertainty using the MC dropout procedure in Algorithm 2, and a gradient update to learning the deep network weights without additional parameters or storage overhead. In addition, the efficiency of Algorithm 2 (MC sample computation) can be improved using parallel batch processing.

#### Algorithm 2 BUNDL Uncertainty Computation from MC Samples

**Require:**  $f_{\theta}(\cdot)$ ,  $x$  from current epoch

**Ensure:** No gradient computation

- 1:  $C \leftarrow \ln 2$ ,  $n \leftarrow 1$ ,  $\bar{f} \leftarrow \mathbf{0} \in \mathbb{R}^N$
- 2: **while**  $n \leq N$  **do**
- 3:    $\bar{f}^n \leftarrow f_{\theta}(x)$  {Network output with dropout}
- 4:    $n \leftarrow n + 1$
- 5: **end while**
- 6:  $\bar{f}_{\theta}(x) \leftarrow \frac{1}{N} \sum_{n=1}^N \bar{f}^n$
- 7:  $z_x^{\hat{y}} \leftarrow \frac{-1}{C \cdot N} \sum_{n=1}^N (\bar{f}^n \log \bar{f}^n + (1 - \bar{f}^n) \log(1 - \bar{f}^n))$

## B. Baseline Comparison Methods

We compare BUNDL with two state-of-the-art approaches for handling noisy training labels. The first approach is Self-Adaptive Learning (SelfAdapt) [40], which uses a weighted sum of given labels and past predictions as a soft-pruning to re-weight and/or leave out noisy samples in loss computation. The second approach is a Noisy Adaptation Layer (NAL) [32], which uses an EM-like algorithm to jointly estimate both clean and noisy label posteriors. We use the “complex model” variant introduced by the authors, as it is better suited for seizure detection. Finally, we include the traditional cross-entropy loss (CEL) as a baseline, which does not account for label noise and implicitly assumes that the provided labels are accurate.

## C. Implementation and Evaluation

As noted above, BUNDL can be used to augment and train any deep network model. To underscore this point, we apply BUNDL to three state-of-the-art networks developed for seizure detection.

- 1) **DeepSOZ:** Our recently-introduced DeepSOZ model [24] consists of a transformer with self-attention that extracts both global features across the EEG channels and channel-wise features for each time window. The global features, representing the patient-level information, are processed by a long short-term memory (LSTM) network, which specializes in modeling temporal dependencies. The LSTM uses these global features to predict the occurrence of seizure activity (i.e., seizure detection). Simultaneously, the channel-wise features are passed through a pooling layer to aggregate information across time for each channel. This pooling allows DeepSOZ to identify the channels most associated with the initiation of seizure activity as the likely onset zone (i.e, seizure localization).
- 2) **TGCN:** The TGCN model introduced by [19] also captures both channel-wise and temporal patterns in EEG data via eight layers of spatio-temporal convolutions (STC). The architecture leverages 1D convolutions that aggregate the EEG data in the neighborhood of each channel. This approach allows TGCN to model the propagation of seizure activity across EEG channels

and time. Following the STC layers, three linear layers are used to refine the extracted features into a binary classification of seizure activity (i.e., seizure detection).

- 3) **CNN:** The CNN model proposed by [23] combines convolutional and recurrent layers to process EEG signals for seizure detection. The CNN component uses 1D convolutions to capture broad temporal features across all EEG channels for each time window. Batch normalization follows the convolutions, which stabilizes the training process. The output is then fed into a bi-directional LSTM (BLSTM) layer, which captures temporal dependencies for reliable seizure detection.

Each of the networks is trained with BUNDL, the noisy label comparison methods (SelfAdapt & NAL), and the baseline CEL. We train the models in a nested 10 fold cross-validation setup, repeated 5 times to have 50 models trained per method. The learning rate is chosen in the range of  $[0.01 - 10^{-6}]$  for each fold by assessing the loss curves in the cross-validation setup. We use Adam optimizer both to pre-train the networks and when augmenting them with the noisy label approaches. Training is done for 30 epochs in the stimulated and TUH datasets and for 50 epochs in CHB dataset (see below for data descriptions). All networks have dropout percentage at 20%. We also use a small tolerance of 0.001 for  $p_g$  to ensure numerical stability. All models are implemented using PyTorch 1.10.

We evaluate the seizure detection performance at two levels. At the window level, we report the area under the receiver operating characteristic curve (AUROC) and the area under the precision-recall curve, which summarize the performance on the individual EEG time windows. At the seizure level, we assess performance across the entire recording and report the percentage of seizures detected, the false positive rate in minutes per hour, and the latency in detecting the seizure onset. The detection threshold for when a predicted probability is considered to be a seizure, is a hyperparameter chosen through nested cross-validation. Specifically, it is selected from the range  $[0.1, 0.8]$  to maximize sensitivity while ensuring a false positive rate of less than 3 minutes/hour on the nested validation dataset.

#### D. SOZ Localization Analysis

While most deep learning methods focus on seizure detection, determining region in which the seizure originates, also known as seizure onset zone (SOZ) localization, is arguably the more important clinical task [50]. For example, if the SOZ can be narrowed to a discrete region in the brain, then surgical resection of this area can provide the highest rate of seizure freedom [50], [51]. DeepSOZ is designed to perform both seizure detection and SOZ localization. We conjecture that the SOZ localization performance is closely tied to its seizure detection accuracy due to the link between the global and channel-wise features. In this study, we analyze the impact of using BUNDL for seizure detection on SOZ localization, as compared to the conventional CEL objective function. We employ 10-fold cross-validation, repeated 5 times, to select the learning rate for training with Adam optimizer in PyTorch 1.10 and to evaluate performance.

#### E. EEG Datasets

**Simulated Data:** We use the SEREEGA framework [52] in MATLAB to simulate EEG data for 120 subjects. We randomly generate between 1 – 10 EEG recordings for each subject ( $5.3 \pm 1.6$  recordings), with each recording lasting 10 minutes. All recordings are sampled in the 10-20 EEG montage at 200 Hz.

Seizure onset and duration are randomly determined for each recording, with seizure durations ranging between 29 – 491 seconds (average  $170 \pm 120.4$  seconds). Outside these seizure intervals, the EEG signals include a background of alpha and beta waves, and

additional noise components that include brief spike noise (5-10 seconds), normal slow waves (5-10 seconds), and Gaussian noise (120-300 seconds) to introduce greater signal complexity. Further details on the EEG data generation are provided below.

- **Seizure Characteristics:** Each subject is assigned a single seizure source characterized by spikes, sharp waves, and polyspike bursts within the 2.5 – 4 Hz range. This source is randomly activated during the seizure period and remains fixed in location for each subject.
- **High-Frequency Noise (Spikes):** High-amplitude one-sided spikes of 6-14Hz are introduced at random times and locations in each recording using the forward model leadfield matrix [53]. The spikes appear as bursts in the 10-20 EEG recordings and span a duration of less than 10 seconds.
- **Low-Frequency Noise (Slow Waves):** One source in the posterior or anterior regions of the brain is assigned to generate slow waves (1 – 3 Hz) in each recording. The duration of these waves is randomly set between 5 – 60 seconds for each subject.
- **Gaussian Noise:** Random bursts of Gaussian noise are applied to all seizure and noise sources, and to two additional sources in the central left and right hemispheres. Gaussian noise is also added 30 seconds before and after seizure onset. Noise is generated at three signal-to-noise ratio (SNR) levels: 3.1 – 6.0 dB, 0.92 – 3.1 dB, and –1.6 – 0.92 dB. SNR levels lower than this would be removed during standard EEG preprocessing.

After generating the 10-20 EEG recordings, we segment the data into 1-second non-overlapping windows. Next, we introduce different types of label noise to simulate faulty seizure annotations for each recording. These include random label errors, over-segmentation of the seizure at 10%, 30% and 50% of the seizure duration, and under-segmentation of the seizure at 10%, 30% and 50% of the seizure duration. If the over-segmentation exceeds the 10-minute recording length, it is truncated to 1 minute outside the true seizure time points. Similarly, we truncate under-segmentation of seizure to at least 29 seconds. As a result, we create 21 variations of the simulated dataset (corresponding to 3 SNR levels  $\times$  7 label noise levels).

**TUH Dataset:** The Temple University Hospital (TUH) corpus is a large publicly available resource, from which we select 120 subjects with focal seizure onset comprising a total of 642 seizure recordings. There are 55 male and 65 female subjects within the age range of 19-91 years ( $55.2 \pm 16.6$ ). Each seizure recording includes average-referenced EEG data from 10-20 montages, along with clinician-labeled seizure intervals and onset channels. We resample the EEG signals to 200 Hz for consistency with the other datasets. We apply minimal preprocessing that includes a bandpass filter (1.6 – 30 Hz) and clipping the signal at two standard deviations from the mean to eliminate high-intensity artifacts in EEG. The EEG signals are standardized to have a zero mean and unit variance using statistics derived from each patient to avoid any information leakage. The recordings are cropped to 10 minutes around the seizure events, while ensuring an even distribution of seizure onset times. The EEG data is then divided into one-second, non-overlapping windows.

For the secondary analysis of SOZ localization, we use the clinician notes to extract the onset channel(s) for each patient in the TUH dataset. This results in 72 seizures originating from the temporal lobe and 48 originating from extra-temporal lobes. There are 59 seizures in the left hemisphere and 61 in the right. While the localization data is not used during detection, it plays a crucial role in epilepsy treatment. Thus, we evaluate how accounting for label noise in the detection task impacts the post-hoc localization performance.

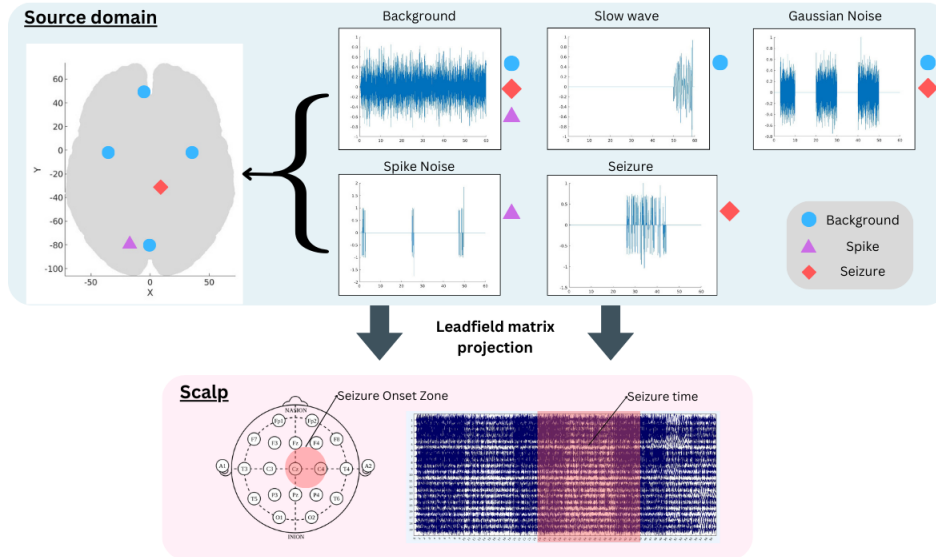


Fig. 3: Pipeline for generating simulated EEG from the seizure and noise sources. Each signal plot is adjacently labeled with its corresponding source type. When a source has more than one signal, all signals are superimposed together before mapping to scalp. The bottom panel shows a scalp plot with a 10-20 montage of electrodes, as generated by the pipeline.

TABLE I: Description of seizure characteristics in simulated, TUH and CHB-MIT datasets.

	Simulated dataset	TUH dataset	CHB-MIT dataset
Number of patients	120	120	23
Total Number of seizures	631	642	181
Average seizures per patient	$5.3 \pm 2.69$	$14.7 \pm 25.2$	$7.9 \pm 6.0$
Min/Max seizures per patient	1/10	1/152	3/27
Average EEG duration per patient	$52.8 \pm 26.97$ min	$79.8 \pm 135$ min	$370 \pm 182.4$
Average seizure duration	$170.5 \pm 120.4$ sec	$88.0 \pm 123.5$ sec	$63.6 \pm 74.0$ sec
Min/Max seizure duration	29/491 sec	7.5/1121 sec	7/753 sec

**CHB Dataset:** The CHB-MIT dataset provides EEG recordings from 23 pediatric subjects (5 male, 17 female) aged 1.5 to 22 years. We use 18 channels from the bipolar-referenced 10-20 montage and resample the data from 256 Hz to 200 Hz. Each 60-minute segment contains at least one seizure, and the dataset includes various seizure types. Patients have between 3 and 27 seizures, averaging  $7.9 \pm 6.0$  minutes in duration, with some exhibiting multiple seizures within a single recording. We apply similar preprocessing steps as for the TUH dataset, which include filtering, artifact removal, signal normalization, and segment the data into 1-second non-overlapping time windows. This standardized approach ensures comparability across datasets and enhances the robustness of our seizure detection models.

## IV. RESULTS

### A. Simulated Experiments

We evaluate the effects of multiple types of label noise when training all three deep network architectures using BUNDL and the baseline noise mitigation strategies. Recall that for simulated data, we have access to the ground-truth seizure labels. We use the noisy labels for model training (as per real-world conditions), but we quantify performance based on the true seizure labels.

Fig. 4 summarizes the performance of each deep network trained using BUNDL and baseline methods across random, over- and under-segmented seizure labels and multiple SNR levels. As seen, BUNDL consistently achieves the best performance across all noise mitigation strategies, as reflected in the window-level metrics of AUROC and AUPRC. In the scenario with randomly noisy labels (rand), characterized by a symmetric mislabeling between the seizure and non-seizure

classes, we observe improved performance at both the window level and seizure level. The application of BUNDL leads to a significantly reduced false positive rate across all three models. The sensitivity and latency also show marginal improvements. The NAL baseline performs comparably to BUNDL, while the SelfAdapt baseline and CEL, which assume no label noise, exhibit lower performance.

Fig. 4 shows the cases in which the seizure class is over-sampled at rates of 10% (over 0.1) and 30% (over 0.3). The cases with 50% over/under-sampling are provided in the appendix. The key challenge for the deep networks is to avoid learning from incorrectly labeled seizure classes, which in turn would lead to false-positive detections. As shown in Fig. 4, BUNDL achieves significantly lower FPR across all models and levels of over-segmented label noise while maintaining comparable sensitivity and latency. The NAL baseline performs second best overall, but its FPR improvement is inconsistent; for instance, with DeepSOZ at over 0.3, the FPR actually increases compared to CEL. SelfAdapt improves FPR and latency but at the cost of reduced sensitivity, indicating that it primarily lowers overall predicted probabilities without effectively addressing label noise.

Finally, we also report the cases in which the seizure class is under-sampled at rates of 10% (under 0.1) and 30% (under 0.3). Once again, the cases with 50% under-sampling is provided in the appendix. Under-segmentation reflects a scenario where clinicians may not fully mark the seizure duration. Hence, the main challenge for the deep networks is to learn seizure characteristics with fewer samples, even under low SNR conditions. BUNDL effectively maintains sensitivity even as training label noise increases from 10% to 30%, showing a significant improvement compared to baseline methods and CEL while maintaining comparable latency and FPR levels. In contrast,

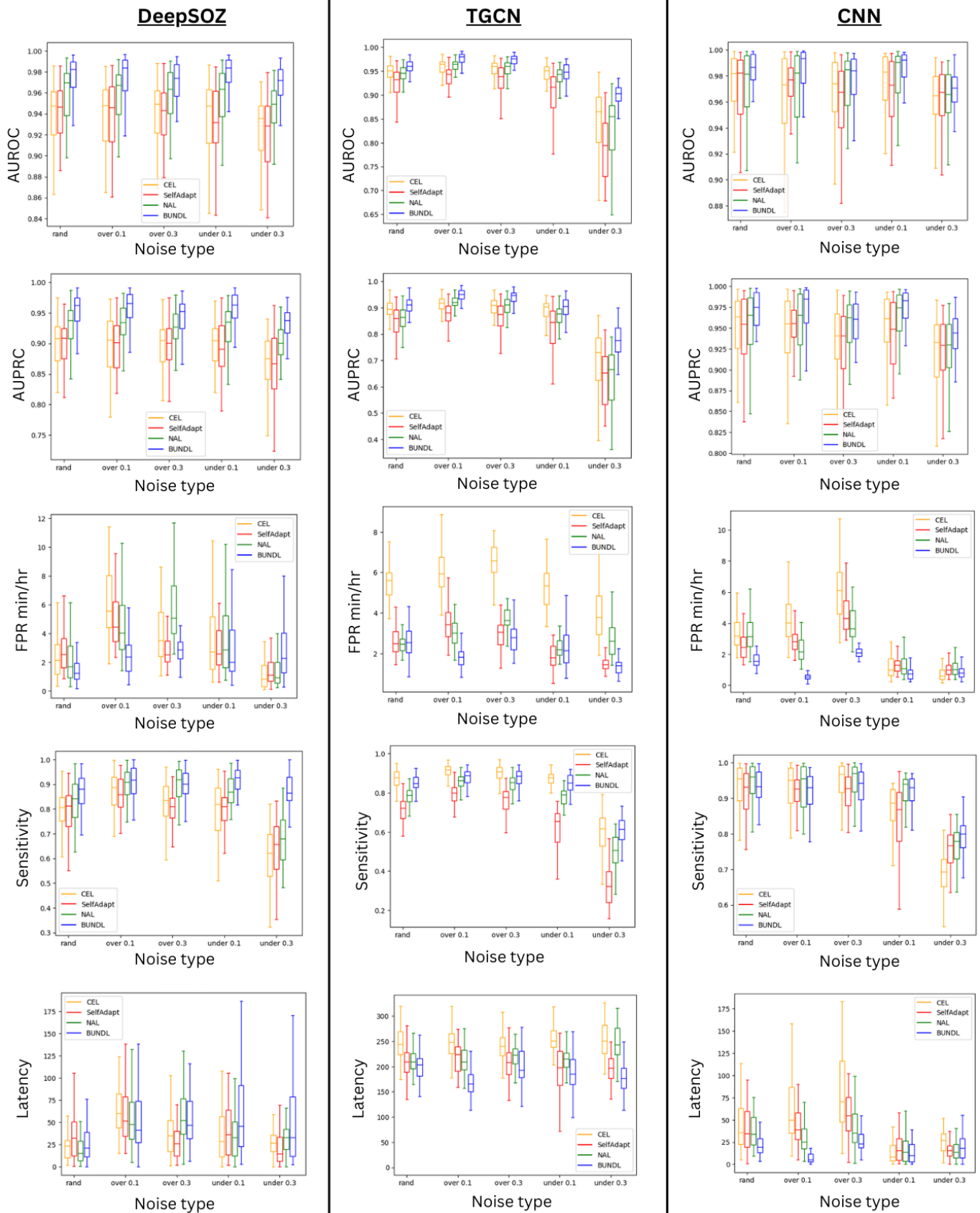


Fig. 4: Box plots of AUROC, FPR (min/hour), and sensitivity metrics of three models trained using BUNDL and baseline strategies at for five different label noise types. Two extreme cases of label noise is provided in appendix.

**TABLE II:** Seizure detection performance based on the DeepSOZ architecture [24] under different noise mitigation strategies on real data.

Dataset	Method	Window-Level		Seizure-Level		
		AUROC	AUPRC	FPR	Sensitivity	Latency
TUH	BUNDL	<b>0.92±0.03</b>	<b>0.60±0.15</b>	<b>2.30±1.10</b>	0.74±0.08	<b>7.6±10.9</b>
	SelfAdapt [40]	0.91±0.03	0.55±0.14	2.50±1.23	0.77±0.07	17.7±14.8
	NAL [32]	0.91±0.03	0.60±0.15	4.24±1.96	<b>0.83± 0.06</b>	22.3± 15.1
	CEL [24]	0.92±0.03	0.60±0.14	3.6±1.77	0.79±0.06	16.9±16.2
CHB-MIT	BUNDL	<b>0.87±0.07</b>	<b>0.33±0.2</b>	<b>1.7±2.9</b>	0.58±0.28	<b>21.54±56.8</b>
	SelfAdapt [40]	0.78±0.12	0.15±0.13	2.2±5.2	0.41±0.30	28.3±47.1
	NAL [32]	0.87±0.09	0.28±0.19	3.4±4.6	0.59±0.28	46.8±94.6
	CEL [24]	0.87±0.09	0.28±0.19	4.4±5.7	<b>0.63±0.23</b>	74.9±169.4

both SelfAdapt and CEL exhibit a substantial drop in sensitivity as label noise levels increase. While NAL shows improvement, it is not significantly better than CEL.

### B. Real World Data

Unlike the simulated data, we do not have access to the ground-truth “clean” seizure labels in the TUH and CHB datasets. Hence, the model performances are evaluated against the clinician-provided (and possibly noisy) labels. In addition, we present the results from training model with the knowledge of over-segmented seizures. This assumption is validated by several articles discussing the pitfalls of inter-rater variability in the datasets [5] and wrong diagnoses of epilepsy due to over segmented seizures [2], [4]. We also focus on the DeepSOZ architecture in this section. The results for the TGCN and CNN architectures are provided in the appendix.

1) *TUH*: Table II (top) summarizes the performance of BUNDL and the baseline noise mitigation strategies using the DeepSOZ architecture. BUNDL demonstrates the best overall performance, as reflected in the AUROC and AUPRC metrics at the window level. At the seizure level, BUNDL achieves a significantly lower false positive rate (FPR) of 2.3 min/hour and a latency of 7.6 seconds, indicating its ability to learn from potentially over-segmented seizures and effectively distinguish ambiguities. In contrast, SelfAdapt has the lowest AUPRC score, coupled with low FPR and sensitivity, suggesting that it primarily increases its overall seizure detection threshold rather than effectively learning from noisy labels. NAL shows comparable performance, but its high sensitivity comes at the cost of a substantially higher FPR of 4.24 min/hour and a latency of 22.3 seconds in seizure detection. CEL, our baseline strategy with no noise assumption, also exhibits a high FPR of 3.6 min/hour.

2) *CHB-MIT*: Table II (bottom) presents the performance comparison between BUNDL and the baseline noise mitigation strategies on the CHB dataset using the DeepSOZ architecture. BUNDL, NAL, and CEL achieve similar mean AUROC scores of 0.87, while SelfAdapt performs poorly at 0.78. We underscore that the CHB dataset differs from the TUH and simulated datasets in two key aspects. First, each recording is one hour long, with patients experiencing between 3 to 27 seizures. Second, the dataset exhibits extreme class imbalance, with only 3% of EEG time points corresponding to seizures. SelfAdapt fails to adjust to this imbalance, resulting in low AUROC and sensitivity close to zero. Given this imbalance, AUPRC is used to emphasize the detection of the minority seizure class through the precision-recall trade-off. BUNDL achieves the highest AUPRC of  $0.33 \pm 0.20$  among all methods. Consistent with results on the TUH and simulated datasets, NAL performs similarly to CEL, which does not account for noise modeling. BUNDL also achieves the lowest

false positive rate of  $1.7 \pm 2.9$  min/hour, with only a minor reduction in sensitivity, whereas both NAL and CEL have over 3 minutes of FPR which is not desirable in a clinical setting.

3) *SOZ localization in TUH*: The DeepSOZ architecture was developed for the dual tasks of seizure detection and onset zone localization [24]. To assess whether accounting for noisy labels enhances the latter task, we trained the localization branch of DeepSOZ after the detection had been trained using BUNDL. This model is compared to naive training of DeepSOZ with CEL, i.e., not accounting for noisy detection labels. At the seizure level, BUNDL achieved an accuracy of  $0.633 \pm 0.149$ , compared to  $0.601 \pm 0.176$  with CEL. At the patient level, where localization predictions are averaged across all recordings for a comprehensive output, BUNDL improved the accuracy from  $0.591 \pm 0.144$  (CEL) to  $0.620 \pm 0.111$ . We hypothesize that the reduction in false positives in seizure detection also reduces false onset zone predictions as seen in two example patients in Fig. 5. This is likely due to the connection between seizure detection and onset zone localization in the attention-based pooling layer of DeepSOZ. Therefore, incorporating BUNDL enhances the overall effectiveness of a dual-task epilepsy monitoring system.

## V. DISCUSSION

We have introduced BUNDL as an effective solution for training deep learning models with noisy labels, specifically as applied to epileptic seizure detection. BUNDL leverages a Monte Carlo (MC) dropout procedure to compute uncertainty and adaptively adjust the loss function during training in the presence of noisy labels. Our extensive analysis using simulated EEG data with artificially introduced noise demonstrates the robustness of BUNDL in identifying noisy samples and in accurately learning true seizure characteristics. We have also applied BUNDL to two real-world EEG datasets (TUH and CHB), and in each case, we demonstrate that BUNDL results in consistent performance improvements. Notably, using BUNDL to improve seizure detection also improves the secondary task of seizure onset localization in the TUH datasets. Taken together, our findings underscore the benefits of BUNDL in enhancing the reliability and utility of automated methods for epilepsy management.

As further validation, we assess the conditional distribution  $p(y/\hat{y}, x)$  given by Eq. (1) to examine the transition from the noisy label  $\hat{y}$  to the true label  $y$  in the BUNDL-DeepSOZ model. This analysis is averaged over data samples centered 60 seconds around seizure onset in  $\hat{y}$ . As shown in Fig. 6 the probability of  $y = 1$  given  $\hat{y} = 0$  for under-segmented seizures in the simulated dataset increases from 0.26 at 10% label noise to 0.38 and 0.45 as the label noise level rises to 30% and 50%, respectively. This observation aligns with the simulation setup, i.e., the seizure duration

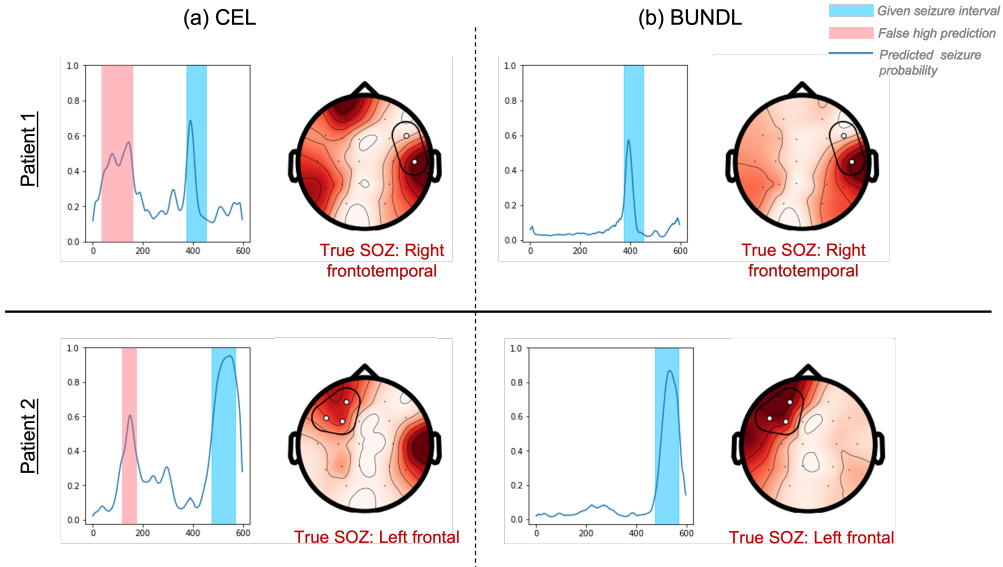


Fig. 5: Temporal seizure prediction (left) and onset zone localization mapped to a topological head plot (right)

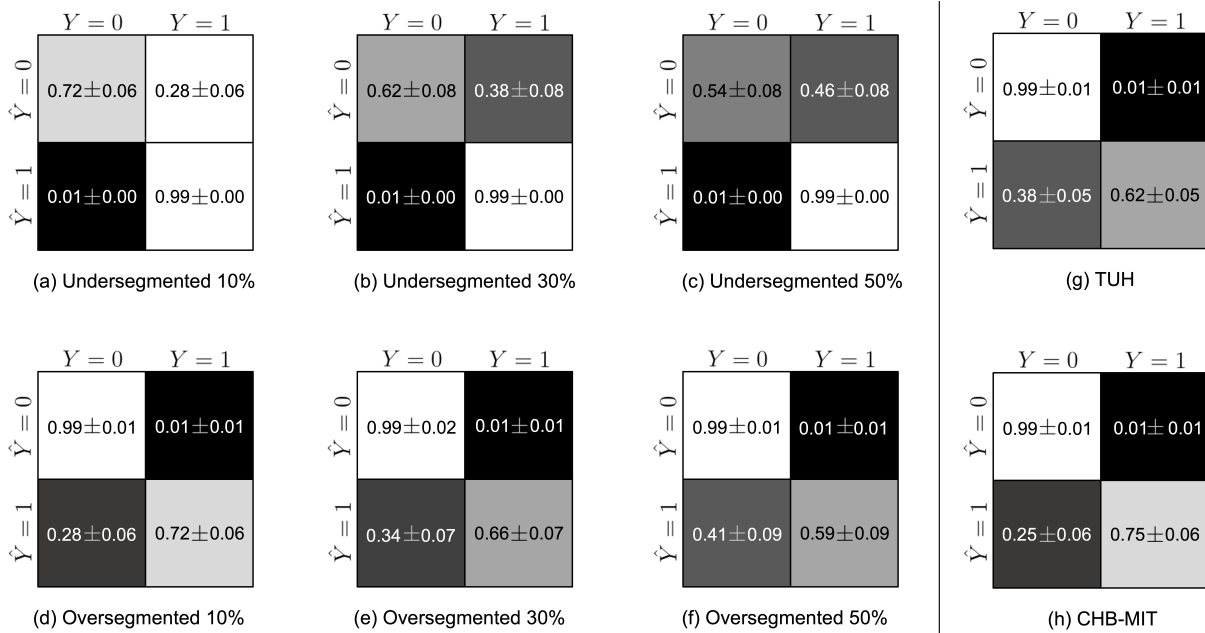


Fig. 6: Transition matrices given by joint probability distribution in six noisy label cases in simulated data and from the real-world datasets.

in  $\hat{y}$  shortens with increasing label noise, meaning more non-seizure points in  $\hat{y}$  overlap with the true seizure  $y$ . Consequently, as label noise increases,  $p(y = 1 | \hat{y} = 0, x)$  also increases. Moreover,  $p(y = 1 | \hat{y} = 1, x)$  remains high because the under-segmented seizure in  $\hat{y}$  exhibits low uncertainty and coincides with the true seizure  $y$ . In contrast, for over-segmented training labels, the non-seizure points in  $\hat{y}$  have low uncertainty by design and align with true non-seizure points in  $y$ , keeping  $p(y = 0 | \hat{y} = 0, x)$  close to 1. However,  $p(y = 1 | \hat{y} = 1, x)$  decreases as label noise increases, since a larger portion of the noisy seizure in  $\hat{y}$  no longer corresponds to the true seizure in  $y$ . BUNDL effectively captures these label mismatches introduced during simulation. In the TUH and CHB datasets, where only noisy labels are available, the predicted distributions exhibit trends consistent with over-segmented seizures. For TUH,  $p(y = 1 | \hat{y} = 1, x)$  is around 0.62, indicating

that approximately 62% of clinician annotations align with true seizures. For CHB, this figure is higher, around 75%, suggesting better annotation quality and cleaner EEG recordings.

We believe the most significant contribution of this work lies in its efficiency and model-agnosticity. BUNDL elegantly utilizes MC dropout, which eliminates the need to add parameters to the original deep neural network. While MC dropout is generally slower than a gradient update, the availability of GPUs during training allows for parallel or batch processing of each forward pass, effectively mitigating the time cost. Moreover, MC dropout is only required during training; during testing, BUNDL operates without any additional steps, maintaining the same efficiency as the traditional cross-entropy loss (CEL) that assumes no noise. Although SelfAdapt offers a similar advantage by avoiding parameter overhead, our simulated and real-world experiments suggest that it fails to effectively handle

noisy labels in complex datasets like EEG. SelfAdapt tends to reduce overall confidence, as it lacks a mechanism for computing uncertainty within the model. In contrast, NAL captures model uncertainty but also introduces parameters to the deep network architecture, which increase quadratically with the number of classes. NAL also modifies the loss function, and the proposed complex model requires three stages of training which is both cumbersome and computationally inefficient. Finally, despite these modification, NAL achieves a lower performance boost than BUNDL in most cases.

One limitation of this work, and of most label noise mitigation strategies, is the reliance on pretraining portions of the model on “clean” data. Pretraining provides an initial approximation that allows the model to begin learning effectively. While BUNDL training combined with Monte Carlo (MC) dropout is designed to mitigate the impact of incorrect features that might have been learned during pretraining, we cannot guarantee that such erroneous features are eliminated and do not impact the prediction. This limitation underscores the importance of starting with a strong initial model, as flaws in the pretrained model could influence the learning process. A promising approach to address this issue could involve the development of more appropriate prior distributions, which better reflect the underlying data characteristics and uncertainties. Additionally, unsupervised or self-supervised pretraining techniques, such as autoencoders or embedding alignment methods using contrastive learning, could be employed before integration with BUNDL. These methods could help the model learn robust and meaningful features without relying on the clinician annotations for feature extraction, thus reducing the risk of learning incorrect patterns during pretraining.

Finally, while this study focuses on the application of BUNDL to EEG data and seizure detection, our strategy is versatile and can be applied to various data types and model architectures. One of BUNDL’s key strengths is its ability to incorporate annotations from multiple raters or clinicians by averaging their scores and incorporating this information into the noisy label distribution parameter. This capability makes BUNDL particularly suitable for medical applications, where inter-rater variability is common and accurate label estimation is crucial. Future work could explore the application of BUNDL to other medical domains that heavily rely on manual annotations, such as medical imaging, pathology, and radiology. Expanding the use of BUNDL to these areas could further demonstrate its utility in enhancing model performance in the presence of noisy or uncertain labels, ultimately contributing to more reliable and generalizable deep learning models in healthcare.

## VI. CONCLUSION

We have introduced BUNDL, a Bayesian strategy to correct for noisy labels when training deep neural networks. By introducing MC dropout and a novel loss function, BUNDL effectively estimates the label uncertainty and adjusts the learning process, reducing the risk of the model adopting incorrect features during training. Our experiments across multiple datasets, including both simulated and real EEG data, consistently demonstrated BUNDL’s ability to improve key performance metrics such as false positive rates, latency, and overall accuracy in seizure detection. Unlike other approaches, BUNDL requires no additional parameter overhead, making it a resource-efficient solution that maintains strong performance. Moreover, BUNDL’s model-agnostic framework is versatile, applicable to various data types and models, offering a robust solution for handling noisy labels across different domains. These contributions highlight the potential of BUNDL to enhance the performance and reliability of deep learning models in critical medical applications.

## AUTHOR CONTRIBUTIONS

AV and DMS conceived and derived the methodology and experimental setup. DMS designed and implemented the simulated data, methodology, evaluation, and visualization. AV and DMS drafted the manuscript. AV was responsible for funding acquisition.

## REFERENCES

- [1] J. J. Halford and et. al., “Standardized database development for eeg epileptiform transient detection: Eegnet scoring system and machine learning analysis,” *Journal of neuroscience methods*, vol. 212, no. 2, pp. 308–316, 2013.
- [2] J. J. Halford and et.al., “Inter-rater agreement on identification of electrographic seizures and periodic discharges in icu eeg recordings,” *Clinical Neurophysiology*, vol. 126, no. 9, pp. 1661–1669, 2015.
- [3] J. Jing and et. al., “Interrater reliability of experts in identifying interictal epileptiform discharges in electroencephalograms,” *JAMA neurology*, vol. 77, no. 1, pp. 49–57, 2020.
- [4] U. Amin and et. al., “The role of eeg in the erroneous diagnosis of epilepsy,” *Journal of Clinical Neurophysiology*, vol. 36, no. 4, pp. 294–297, 2019.
- [5] L. A. Gemein and et. al., “Machine-learning-based diagnostics of eeg pathology,” *NeuroImage*, vol. 220, p. 117021, 2020.
- [6] R. K. Joshi and et. al., “Spatiotemporal analysis of interictal eeg for automated seizure detection and classification,” *Biomedical Signal Processing and Control*, vol. 79, p. 104086, 2023.
- [7] D. Wu and et. al., “Automatic epileptic seizures joint detection algorithm based on improved multi-domain feature of ceeg and spike feature of aeeg,” *IEEE Access*, vol. 7, pp. 41 551–41 564, 2019.
- [8] S. Nesaee and et. al., “Real-time detection of precursors to epileptic seizures: Non-linear analysis of system dynamics,” *Journal of Medical Signals & Sensors*, vol. 4, no. 2, pp. 103–112, 2014.
- [9] J. Craley and et. al., “A novel method for epileptic seizure detection using coupled hidden markov models,” in *Medical Image Computing and Computer Assisted Intervention—MICCAI 2018: 21st International Conference, Granada, Spain, September 16–20, 2018, Proceedings, Part III 11*. Springer, 2018, pp. 482–489.
- [10] S. Liu and et. al., “Epileptic seizure detection and prediction in eegs using power spectra density parameterization,” *IEEE Transactions on Neural Systems and Rehabilitation Engineering*, 2023.
- [11] K. Samiee and et. al., “Epileptic seizure classification of eeg time-series using rational discrete short-time fourier transform,” *IEEE transactions on bio-medical engineering*, vol. 62, no. 2, pp. 541–552, 2015.
- [12] A. S. Zandi and et. al., “Automated real-time epileptic seizure detection in scalp eeg recordings using an algorithm based on wavelet packet transform,” *IEEE Transactions on Biomedical Engineering*, vol. 57, no. 7, pp. 1639–1651, 2010.
- [13] B. Akbarian and et. al., “A framework for seizure detection using effective connectivity, graph theory, and multi-level modular network,” *Biomedical Signal Processing and Control*, vol. 59, p. 101878, 2020.
- [14] F. Hassan and et. al., “Epileptic seizure detection using a hybrid 1d cnn-machine learning approach from eeg data,” *Journal of Healthcare Engineering*, vol. 2022, no. 1, p. 9579422, 2022.
- [15] H. S. Nogay and et. al., “Detection of epileptic seizure using pretrained deep convolutional neural network and transfer learning,” *European neurology*, vol. 83, no. 6, pp. 602–614, 2021.
- [16] G. Choi and et. al., “A novel multi-scale 3d cnn with deep neural network for epileptic seizure detection,” in *2019 IEEE International Conference on Consumer Electronics (ICCE)*. IEEE, 2019, pp. 1–2.
- [17] N. Wagh and et. al., “Eeg-gcnn: Augmenting electroencephalogram-based neurological disease diagnosis using a domain-guided graph convolutional neural network,” in *Machine Learning for Health*. PMLR, 2020, pp. 367–378.
- [18] X. Chen and et. al., “Multi-dimensional enhanced seizure prediction framework based on graph convolutional network,” *Frontiers in Neuroinformatics*, vol. 15, p. 605729, 2021.
- [19] I. C. Covert and et. al., “Temporal graph convolutional networks for automatic seizure detection,” in *Machine Learning for Healthcare*. PMLR, 2019, pp. 160–180.
- [20] N. F. Güler and et. al., “Recurrent neural networks employing lyapunov exponents for eeg signals classification,” *Expert systems with applications*, vol. 29, no. 3, pp. 506–514, 2005.
- [21] L. Vidyaratne and et. al., “Deep recurrent neural network for seizure detection,” in *2016 International Joint Conference on Neural Networks (IJCNN)*. IEEE, 2016, pp. 1202–1207.

- [22] X. Hu and et. al., "Scalp eeg classification using deep bi-lstm network for seizure detection," *Computers in Biology and Medicine*, vol. 124, p. 103919, 2020.
- [23] J. Craley and et. al., "Automated inter-patient seizure detection using multichannel convolutional and recurrent neural networks," *Biomedical signal processing and control*, vol. 64, p. 102360, 2021.
- [24] D. M. Shama and et. al., "Deepsoz: A robust deep model for joint temporal and spatial seizure onset localization from multichannel eeg data," in *International Conference on Medical Image Computing and Computer-Assisted Intervention*. Springer, 2023, pp. 184–194.
- [25] R. Hussein and et. al., "Multi-channel vision transformer for epileptic seizure prediction," *Biomedicine*, vol. 10, no. 7, p. 1551, 2022.
- [26] C. Li and et. al., "Eeg-based seizure prediction via transformer guided cnn," *Measurement*, vol. 203, p. 111948, 2022.
- [27] J. Pedoeem and et. al., "Tabs: Transformer based seizure detection," in *Biomedical Sensing and Analysis: Signal Processing in Medicine and Biology*. Springer, 2022, pp. 133–160.
- [28] P. Chen and et. al., "Understanding and utilizing deep neural networks trained with noisy labels," PMLR, 2019, pp. 1062–1070.
- [29] D. Park and et. al., "Robust data pruning under label noise via maximizing re-labeling accuracy," *arXiv preprint arXiv:2311.01002*, 2023.
- [30] C. Northcutt and et. al., "Confident learning: Estimating uncertainty in dataset labels," *Journal of Artificial Intelligence Research*, vol. 70, pp. 1373–1411, 2021.
- [31] C. Xue and et. al., "Robust learning at noisy labeled medical images: Applied to skin lesion classification," in *2019 IEEE 16th International Symposium on Biomedical Imaging (ISBI 2019)*. IEEE, 2019, pp. 1280–1283.
- [32] J. Goldberger and et. al., "Training deep neural-networks using a noise adaptation layer," in *International conference on learning representations*, 2016.
- [33] S. Sukhbaatar, "Training convolutional networks with noisy labels," *arXiv preprint arXiv:1406.2080*, 2014.
- [34] Y. Zhang and et. al., "Learning noise transition matrix from only noisy labels via total variation regularization," in *International Conference on Machine Learning*. PMLR, 2021, pp. 12501–12512.
- [35] Z. Wen and et. al., "Histopathology image classification with noisy labels via the ranking margins," *IEEE Transactions on Medical Imaging*, 2024.
- [36] Z. Xu and et. al., "Anti-interference from noisy labels: Mean-teacher-assisted confident learning for medical image segmentation," *IEEE Transactions on Medical Imaging*, vol. 41, no. 11, pp. 3062–3073, 2022.
- [37] J. Chen and et. al., "Label-retrieval-augmented diffusion models for learning from noisy labels," *Advances in Neural Information Processing Systems*, vol. 36, 2024.
- [38] Z. Hailat and et. al., "Teacher/student deep semi-supervised learning for training with noisy labels," in *2018 17th IEEE International Conference on Machine Learning and Applications (ICMLA)*. IEEE, 2018, pp. 907–912.
- [39] T. Xiao and et. al., "Learning from massive noisy labeled data for image classification," in *Proceedings of the IEEE conference on computer vision and pattern recognition*, 2015, pp. 2691–2699.
- [40] L. Huang and et. al., "Self-adaptive training: beyond empirical risk minimization," *Advances in neural information processing systems*, vol. 33, pp. 19365–19376, 2020.
- [41] E. Arazo and et. al., "Unsupervised label noise modeling and loss correction," in *International conference on machine learning*. PMLR, 2019, pp. 312–321.
- [42] X.-C. Li and et. al., "Dynamics-aware loss for learning with label noise," *Pattern Recognition*, vol. 144, p. 109835, 2023.
- [43] Z. Zhang and et. al., "Generalized cross entropy loss for training deep neural networks with noisy labels," *Advances in neural information processing systems*, vol. 31, 2018.
- [44] Y. Qiu and et. al., "Denosing sparse autoencoder-based ictal eeg classification," *IEEE Transactions on Neural Systems and Rehabilitation Engineering*, vol. 26, no. 9, pp. 1717–1726, 2018.
- [45] A. Borovac and et. al., "Calibration of automatic seizure detection algorithms," in *2022 IEEE Signal Processing in Medicine and Biology Symposium (SPMB)*. IEEE, 2022, pp. 1–6.
- [46] C. Li and et. al., "Eeg-based seizure prediction via model uncertainty learning," *IEEE Transactions on Neural Systems and Rehabilitation Engineering*, vol. 31, pp. 180–191, 2022.
- [47] G. Segal and et. al., "Utilizing risk-controlling prediction calibration to reduce false alarm rates in epileptic seizure prediction," *Frontiers in Neuroscience*, vol. 17, p. 1184990, 2023.
- [48] K. Saab and et. al., "Weak supervision as an efficient approach for automated seizure detection in electroencephalography," *NPJ digital medicine*, vol. 3, no. 1, p. 59, 2020.
- [49] A. Borovac and et. al., "Ensemble learning using individual neonatal data for seizure detection," *IEEE journal of translational engineering in health and medicine*, vol. 10, pp. 1–11, 2022.
- [50] F. Rosenow and et. al., "Presurgical evaluation of epilepsy," *Brain*, vol. 124, no. 9, pp. 1683–1700, 2001.
- [51] S. Olmi and et. al., "Controlling seizure propagation in large-scale brain networks," *PLoS computational biology*, vol. 15, no. 2, p. e1006805, 2019.
- [52] L. R. Krol and et. al., "Sereega: Simulating event-related eeg activity," *Journal of neuroscience methods*, vol. 309, pp. 13–24, 2018.
- [53] Y. Huang and et. al., "The new york head—a precise standardized volume conductor model for eeg source localization and tes targeting," *NeuroImage*, vol. 140, pp. 150–162, 2016.

## APPENDIX I ADDITIONAL RESULTS

### A. Extreme Label Noise:

Fig 7 summarises performance across the three architectures for the different noise mitigation strategies and *high* levels of label noise (50% over-segmentation and under-segmentation). We also plot the symmetric noise (rand) for comparison. In over-segmented dataset, even at extreme cases training all three models with BUNDL does not deteriorate metrics significantly and it outperforms all baselines. In under-segmented dataset, although BUNDL still outperforms all baselines in all three models, the performance gain is only significant in DeepSOZ architecture. In TGCN and CNN, all methods result in poor sensitivity, which can be attributed to extreme imbalance of classes in the labels i.e., there are very few seizure annotations to learn from. This suggests model fragility in TGCN and CNN.

### B. Effect of SNR

To evaluate the effect of signal-to-noise ratio (SNR) on model performance, we had introduced Gaussian noise at three different amplitude levels during the creation of our simulated dataset. We show AUROC metric obtained from repeated 10-fold cross-validation under conditions of randomly segmented seizure label noise. This noise configuration was chosen due to its minimal assumptions. Our results shown in Figure ( 8 demonstrate that the median AUROC for all three models remains consistently high across varying SNR levels when trained with BUNDL. In contrast, models trained using the two baseline methods and CEL exhibit a gradual decline in AUROC as the SNR increases, a trend that is pronounced in the DeepSOZ and TGCN models. BUNDL, however, has better performance in all scenarios. Further, the we also observe that FPR significantly increases for baseline methods with decreasing SNR, with slight decrease in sensitivity. BUNDL on the other hand, achieves the least FPR while maintaining comparable sensitivity. These findings underscore the robustness of BUNDL in maintaining superior performance despite increased noise interference in the data.

### C. Additional architectures on real world dataset

Table III summarizes the seizure-level performance of two additional architectures (TGCN and CNN) on the TUH and CHB-MIT datasets trained with different noise mitigation strategies. Window-level metrics are omitted as they are largely similar across methods. A similar trend as DeepSOZ is observed. In both datasets, BUNDL achieves the least latency and FPR. In TUH, SelfAdapt and CEL perform similarly, while NAL yields high sensitivity but at the cost of higher FPR and latency. In CHB-MIT, CEL has the highest sensitivity but poor FPR and latency. NAL performs well with TGCN, but SelfAdapt leads to high FPR, whereas in CNN, the reverse is true resulting in higher FPR with NAL and lower with Selfadapt. This indicates that the baselines have poor generalizability across datasets and architectures, with BUNDL providing stable performance with low FPR, latency, and comparable sensitivity.

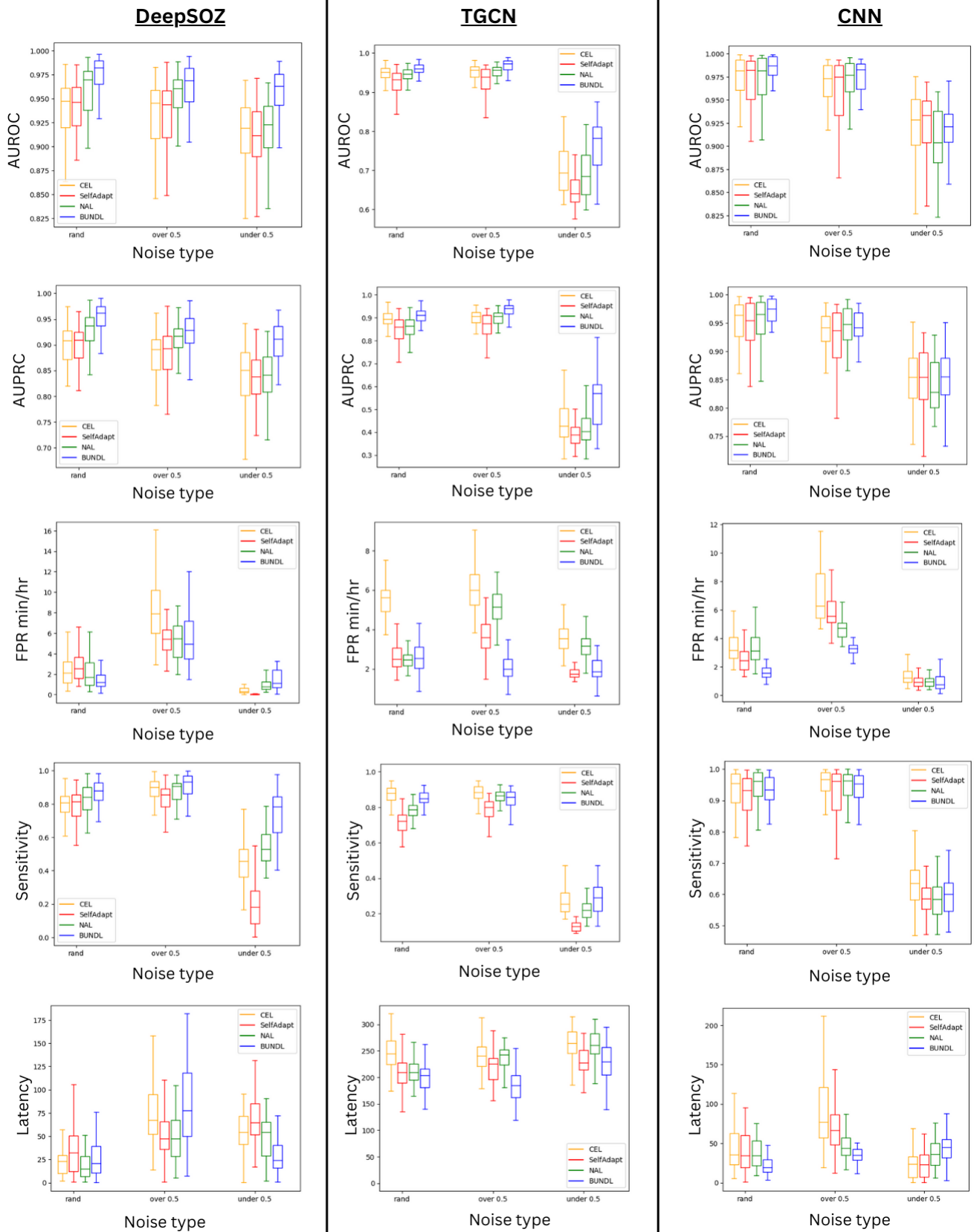


Fig. 7: Box plots of AUROC, FPR (min/hour), and sensitivity metrics of three models trained using BUNDL and baseline strategies at symmetric noise case (rand) compared against extreme cases of over-segmentation and under-segmentation at 50% of seizure length.

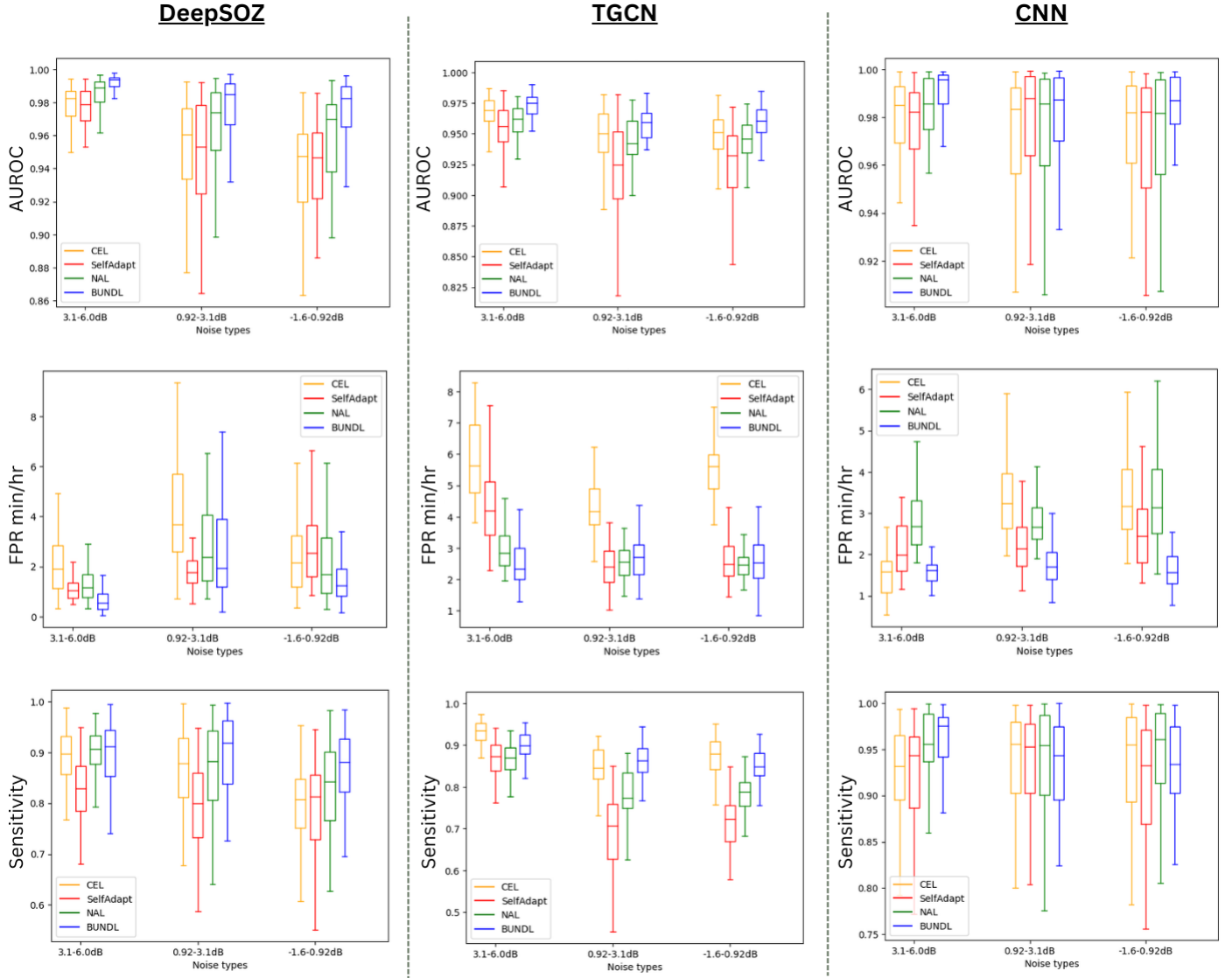


Fig. 8: Box plots of AUROC, FPR (min/hr), and sensitivity metrics of three models trained using BUNDL and baseline strategies at three different SNR levels and randomly noisy training labels.

TABLE III: Comparison of BUNDL and baseline methods using additional two state-of-the-art architectures across two datasets. Seizure level metrics are reported here.

Architecture	Method	TUH			CHB-MIT		
		FPR	Sensitivity	Latency	FPR	Sensitivity	Latency
TGCN	BUNDL	<b>2.6±2.5</b>	0.75±0.09	<b>30.1±29.7</b>	<b>0.8±1.8</b>	0.71±0.29	<b>14.7±11.6</b>
	Selfadapt	3.0±1.2	0.81±0.08	41.2±17.3	2.6±8.1	0.75±0.26	51.9± 264.2
	NAL	2.8±1.5	<b>0.87±0.07</b>	50.4±28.5	<b>0.8±0.3</b>	0.77±0.24	18.1±12.2
	CEL	3.3±1.6	0.84±0.06	41.3±19.5	3.2±1.0	<b>0.83±0.23</b>	33.7±19.8
CNN	BUNDL	<b>2.7±3.5</b>	0.54±0.23	<b>11.2±28.9</b>	<b>0.8±0.7</b>	0.64±0.33	<b>10.2±11.6</b>
	Selfadapt	3.4±1.9	0.66±0.09	15.7±16.1	1.0±0.7	0.67±0.33	11.0±7.0
	NAL	5.6±3.3	<b>0.85±0.11</b>	43.7±33.0	2.6±2.3	0.72±0.31	21.8±15.5
	CEL	3.0±2.2	0.66±0.13	15.5±20.1	2.7±1.2	<b>0.76±0.28</b>	28.7±82.3